16th World Conference on Earthquake, 16WCEE 2017

Santiago Chile, January 9th to 13th 2017

Paper N° 4528

Registration Code: S-W1467238207

ACCOUNTING FOR SOIL-STRUCTURE INTERACTION IN THE SEISMIC DESIGN OF RC WALL STRUCTURES ON SHALLOW FOUNDATIONS

D. Sotiriadis [(1)], A. A. Correia [(2)], T. J. Sullivan [(3)]

[(1)] *M.Sc. Student, MEEES Programme, UME School, IUSS Pavia, Pavia, d.sotiriadis@meees.org*
[(2)] *Postdoctoral Researcher, National Laboratory for Civil Engineering, Lisbon, aacorreia@lnec.pt*
[(3)] *Associate Prof., Dept. of Civil and Natural Resources Eng., Univ. of Canterbury, Christchurch, timothy.sullivan@canterbury.ac.nz*

Abstract

The research findings made in recent years now mean that the prospect of accounting for soil-foundation-structure interaction within seismic design is becoming a viable reality. By examining the cyclic response of a parameterized set of shallow foundations, simulated using a recently developed macro-element model that accounts for rotational-vertical-horizontal motion interaction and which considers coherently possible uplift behaviour, new degradation curves for the stiffness and damping of shallow foundations are developed. The improvements included in these curves with respect to previous proposals are: i) the uplift mechanism, a non-dissipative nonlinear mechanism, is taken into account and ii) the overturning moment and the corresponding simultaneous horizontal load are applied on the footing so that the effect of shear force on the overall response is investigated.

It is found that rotational stiffness degradation is more severe when shear demands are relatively large compared to flexural demands. Moreover, the stiffness degradation becomes more intense as the static factor of safety for centred vertical loads on the foundation reduces, since the response tends to be dominated by hysteretic behaviour in contrast to an increasingly rigid-body rocking response for larger factors of safety. Hysteretic energy dissipation evolution is represented via equivalent viscous damping curves, obtained from quasi-static cyclic analyses.

Finally, the new set of stiffness and damping curves are included for use within the direct displacement-based design framework. By using the improved curves, the bearing capacity of the foundation will be automatically respected since each point of the developed curves will correspond to a solution lying inside or on the ultimate load surface of the foundation system. The benefit of this approach is illustrated through the design of 6-, 8- and 12-storey buildings with and without taking into consideration soil-foundation-structure interaction. Nonlinear dynamic analyses are used to gauge the performance of the design solutions, and it is found that, even though the prediction of foundation rotation demands can be further improved, the direct displacement-based design method provides good control of storey drifts and displacements, suggesting that it could be a valuable procedure for performance-based earthquake engineering in the future.

Keywords: RC wall structure; soil-foundation-structure interaction; shallow foundation; direct displacement-based design

1. Introduction

Displacements and deformations are closely related to the damage exhibited by structures under strong seismic excitation. Direct displacement-based design (DDBD) was proposed by Priestley *et al*. [1] as an effective method for controlling displacements in the seismic design of structures, which is particularly important for performance-based design (PBD). The increasing interest of the earthquake engineering community in PBD, has led to a greater consideration of the role played by soil-foundation-structure interaction (SFSI) on the overall behaviour of structural systems.

Traditionally, seismic design codes would rely only on the superstructure to deform inelastically in order to dissipate seismic energy. However, current seismic design codes, while forbidding damage to occur in the foundation elements, in certain cases already allow for limited permanent deformations at the soil-foundation system. As shown by several researchers (e.g., Mylonakis and Gazetas [2]), nonlinear foundation response is almost unavoidable in many practical cases, since overturning moments at the foundation base may become temporarily larger than the foundation static bearing capacity during an earthquake. In this case, the nonlinear foundation response may absorb an important part of the seismic input energy, lowering the seismic demands on the superstructure. This type of behaviour has been claimed to be an efficient seismic design strategy, especially for retrofitting existing structures where a foundation has responded nonlinearly during past earthquakes and any rehabilitation effort would be too expensive and difficult. The idea to exploit nonlinear energy dissipation at the soil-foundation interface is thus becoming more and more attractive and has already led to a number of research efforts where the inelastic response of the foundation subsoil is investigated as well as its effects on the superstructure [2-8]. Furthermore, the same concept has led to some outstanding examples of seismic design of foundations allowed to uplift or slide during earthquakes such as the case of the Rion-Antirion cable-stayed bridge in Greece (Pecker [9]).

Important research findings during the past 20 years [5, 10-16] have contributed to the development of efficient SFSI macro-element models whose accuracy is comparable with that of complex finite element models but whose computational cost is relatively low. This has allowed researchers such as Paolucci *et al*. [17] to conduct numerous parametric analyses and to develop design tools accounting for SFSI. Therefore, controlled foundation uplift and/or controlled plastic response of soil-foundation systems are expected soon to become a "rational" and economically efficient earthquake protection solution which will lead to new PBD approaches including nonlinear SFSI [7].

In light of the above, the work presented herein aims to develop a reliable framework for considering SFSI within a DDBD approach for reinforced concrete wall structures. Achieving this objective will result in an integral design procedure where both the superstructure and the foundation are simultaneously designed and the interaction between them is taken into account.

2. Accounting for SFSI in DDBD

The first considerations of SFSI within a DDBD approach appear to have been presented by Priestley [18] and Priestley *et al*. [1], where the system yield and design displacement were adjusted to account for the displacement coming from the foundation rotation. The impact of the foundation deformability depends on whether the design displacement is governed by material strain or storey drift limits. In the case where material strains govern, the total design displacement for a given limit state will be increased by an amount roughly equal to the rigid-body displacement corresponding to the foundation rotation and, consequently, the system effective stiffness will decrease. Nevertheless, in this case the ductility demand and equivalent viscous damping of the superstructure will be approximately the same as the one resulting from a fixed-base design and so the required design strength will potentially tend to decrease. On the other hand, where the design displacement is instead governed by storey drift limits the system design displacement will remain essentially the same, while the foundation deformability will lead to a decrease in the allowable ductility demand on the superstructure, thus requiring more strength to maintain the storey drift limits.

A means of accounting for the influence of damping due to hysteretic response of the soil beneath the foundation within a DDBD procedure was proposed by Priestley *et al*. [1]. If the foundation damping, ξ_f, is

known, it can be combined with a damping component associated with inelastic response of the superstructure, ξ_s, to give the system damping ratio, ξ_{sys}, as shown in the following equation:

$$\xi_{sys} = \frac{\xi_f \Delta_f + \xi_s \Delta_s}{\Delta_f + \Delta_s} \quad (1)$$

In this equation, Δ_f and Δ_s are the displacement components of the SDOF system due to foundation and superstructure deformations respectively. This approach approximates the shear in the foundation and superstructure as being equal and hence weighs different damping components by their elastic strain energy proportions. The effect of SFSI on the representation of the system as a SDOF is illustrated in Fig. 1.

Paolucci *et al*. [17] proposed an iterative design procedure aimed at explicitly introducing nonlinear SFSI in DDBD. The procedure is based on the use of empirical curves quantifying the foundation stiffness degradation, K_f / K_{f0}, and the corresponding EVD ratio, ξ_f, as a function of foundation rotation. The design procedure starts with an initial foundation design followed by an assumption on the amplitude of foundation rotation. During the design procedure the foundation rotation is iteratively computed until convergence in terms of stiffness degradation, damping and foundation rotation is achieved. At the end of the design, the bearing capacity of the foundation is checked so that the feasibility of the solution is verified.

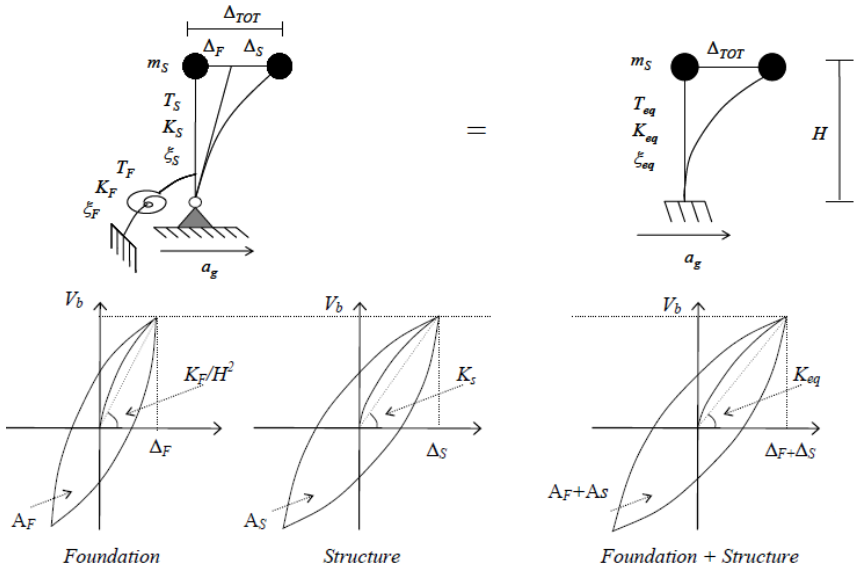

Fig. 1: Representation of SDOF oscillator including SFSI and its effect on system effective stiffness and equivalent viscous damping (adapted from Priestley et al., 2007)

Sullivan *et al*. [19] developed the methodology for RC wall systems on shallow foundations, proposing a slightly modified design procedure so that the engineer establishes the desired foundation performance at the beginning of the design process and thus determines the required properties of the foundation. If the foundation size needs to be minimized, a large allowable foundation rotation should be designed for whereas a larger size results when the foundation is not permitted to deform substantially. In Fig. 2, the flowchart of the design procedure proposed by Sullivan *et al*. [19] is presented as it will be developed and applied herein.

3. Response of shallow foundations

The design procedures of Paolucci *et al*. [17] and Sullivan *et al*. [19] make reference to a set of empirical curves developed in [17] to describe the foundation secant stiffness degradation and EVD ratio as a function of foundation rotation. The curves were developed through cyclic, quasi-static analyses of footing elements using the macro-element developed by di Prisco *et al*. [11]. In their analyses, Paolucci *et al*. [17] included only the rotational degree of freedom of the foundation element on which only vertical and moment loading was applied.

In addition to this, the uplift mechanism, i.e., the partial detachment of the footing from the soil, was not included in those analyses.

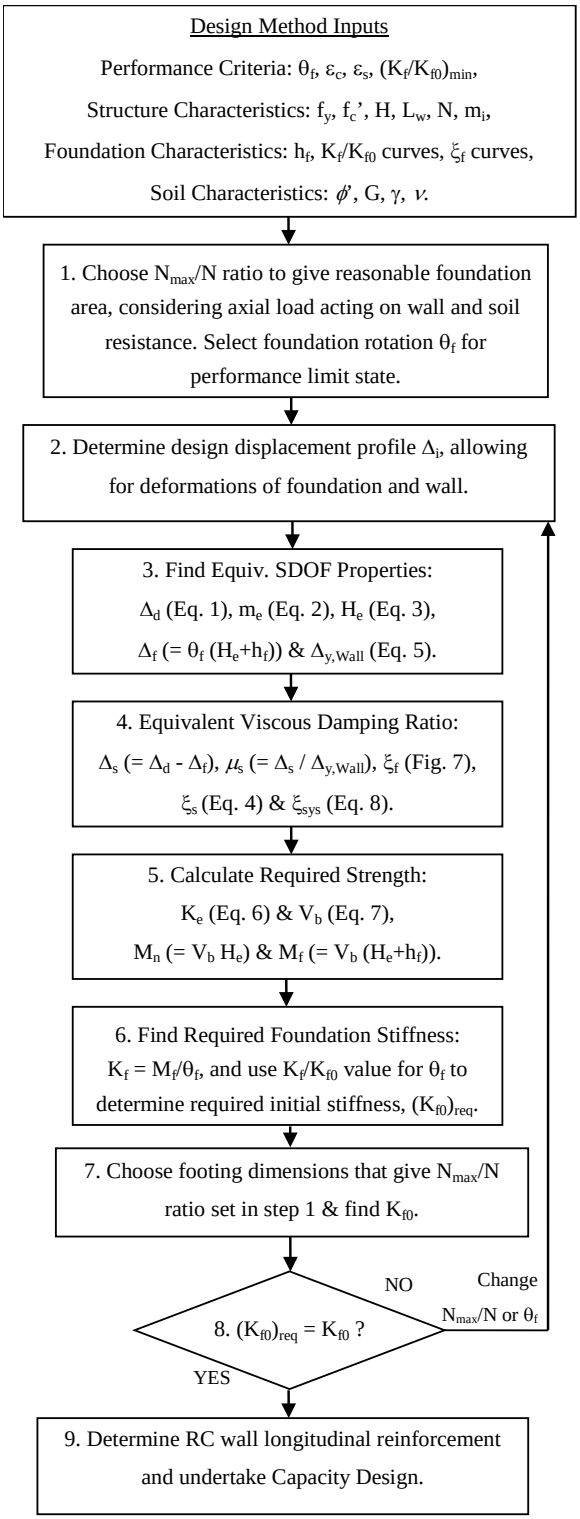

Fig. 2: Schematic flowchart of iterative DDBD procedure accounting for SFSI (adapted from [19])

An important objective of the effort presented herein is to further investigate the response of shallow foundations under quasi-static cyclic loading by considering simultaneously vertical and horizontal loads as well

as overturning moments acting on a footing. The ultimate goal is to produce stiffness degradation and EVD ratio curves, similar to the ones developed in [17]. However, the main differences between the curves produced herein and the existing ones are: i) the uplift mechanism, a non-dissipative nonlinear mechanism, is taken into account and ii) the overturning moment and the corresponding simultaneous horizontal load are applied on the footing so that the effect of shear force and footing sliding on the overall response is investigated. The aforementioned improvements will have a direct impact on the DDBD procedure accounting for nonlinear SFSI described earlier; consideration of uplift and loading conditions will be improved and the feasibility of each foundation solution will automatically respect the bearing capacity expression (in contrast to the approach of [17]) since each point of the developed curves will correspond to a solution lying inside or on the ultimate load surface of the foundation system.

The derivation of these curves is performed through the use of a recent SFSI macro-element model developed by Correia *et al*. [20], which was implemented in SeismoStruct [21]. The macro-element framework for shallow foundations has been developed by the earthquake engineering community during the last 15 years, and is now frequently adopted in research studies that require a reliable estimation of soil-foundation displacements. These models have previously shown to be a cost-effective tool for such type of analysis, since they suitably represent both the nonlinear soil behaviour at near-field and the ground substratum dynamic characteristics at far-field, as well as the interaction with the seismic response of the structure.

The macro-element model by Correia *et al*. [20] builds upon the innovative concepts and formulations of the models by Chatzigogos *et al*. [14, 15] and by Figini *et al*. [16]. Nevertheless, it incorporates some major improvements, namely addressing inconsistencies regarding the formulation of the participating mechanisms and extending their scope to three-dimensional loading cases. Moreover, this macro-element introduces a significantly enhanced uplift model, based on a nonlinear elastic-uplift response which also considers some degradation of the contact at the soil/footing interface due to irrecoverable changes in its geometry. An improved bounding surface plasticity model is also adopted in order to reproduce a more general and realistic behaviour, which correctly takes into account the simultaneous elastic-uplift and plastic nonlinear responses. Finally, the soil type considered herein is medium dense sand and, therefore, the “rugby ball” shaped ultimate load surface of [10] is adopted.

3.1 Stiffness degradation curves for cyclic loading

A square footing with 7.5 m side dimension was adopted in this study, which was supported on sand with a friction angle of 33.5˚, shear modulus of 90 MPa and Poisson’s ratio of 0.3. The corresponding footing bearing capacity under pure vertical load was 40 MN. However, it should be noted that non-dimensional quantities were used for developing K_f / K_{f0} degradation and ξ_f curves. Consequently, the particular footing geometry and soil characteristics described above do not affect the results obtained herein. Nevertheless, based on the parameter values that were chosen, the curves presented herein are valid for square, rigid footings lying on medium dense to dense sand. The initial stiffness properties of the footing were calculated based on well-known expressions of foundation impedances for square footings (e.g., Mylonakis *et al*. [22]).

The structural model that was used in order to perform the analyses consists of a footing macro-element, with fully coupled degrees of freedom, which supports a rigid frame element representing the superstructure. At the top of the frame element, a quasi-static cyclic horizontal displacement loading in one direction was imposed in addition to the vertical load. P-Δ effects were also taken into account.

The main parameters affecting the secant stiffness degradation of a surface footing are: i) the static safety factor (*SF*) for a centred vertical load, corresponding to the ratio of the bearing capacity of the footing, N_{max}, to the applied vertical load, *N*, and ii) the ratio of the effective height of the superstructure H_e to the foundation width *B*. Therefore, this parametric study considered six values of *SF* and four values of H_e / B.

It should be noted that all degrees of freedom of the footing element in the loading plane were kept free so that the results include effects of both sliding and uplift. The effect of sliding mechanism is expected to be more pronounced for low values of H_e / B whereas the effect of uplift mechanism is expected to be dominant for large *SF* values and highly affected by the geometric properties of the footing. However, the objective of this research is to derive general rotational stiffness degradation curves which will not depend directly on the foundation

particular dimensions. In order to normalize the effect of uplift on the results, it was deemed appropriate to provide the stiffness degradation (K_f / K_{f0}) with respect to the foundation rotation normalized by the rotation of uplift initiation (θ_f / θ_{up}). By doing this, the resulting curves can be grouped just in terms of *SF* and H_e / B. However, it is noted that this normalization does not include the effect of footing shape, which should be evaluated as well. The normalized moment of uplift initiation (the point at which the first edge detaches from the soil) is calculated, according to the formulation of the macro-element [20], as:

$$Q_{Mup} = \frac{M_{up}}{N_{max} B} = \frac{1}{2\alpha(1+Q_N)} Q_N, \quad with \quad Q_N = \frac{N}{N_{max}} = \frac{1}{SF} \tag{2}$$

Consequently, the rotation of uplift initiation is calculated as:

$$\theta_{up} = \frac{M_{up}}{K_{f0}} = \frac{N_{max} B}{2\alpha\, K_{f0}\, (1+SF)} \tag{3}$$

In the previous expressions: Q_{Mup} is the normalized moment of uplift initiation; Q_N is the normalized vertical load (corresponding to the inverse of *SF*); and α is the uplift initiation parameter. The latter can be determined from simple static considerations and is only dependent on the assumed stress distribution of vertical stresses underneath the foundation – it is equal to 3 if a linear distribution of vertical stresses underneath the foundation is assumed for the soil at the beginning of the analysis [20].

After all the quasi-static cyclic analyses had been run, the normalized rotation and stiffness values (θ_f / θ_{up}, K_f / K_{f0}) were plotted and a function was fit to them. The shape of that function was taken equal to the one from Paolucci *et al*. [17] and is shown below:

$$\frac{K_f}{K_{f0}} = \frac{1}{1+a\left(\frac{\theta_f}{\theta_{up}}\right)^b} \tag{4}$$

In Fig. 3, the stiffness degradation curves, obtained after calibrating the parameters *a* and *b*, are presented for a wide range of *SF* values and for geometric ratios H_e / B equal to 1, 2 and 3. For H_e / B greater than 3 the shear force does not significantly affect the stiffness degradation of a square footing, due to insignificant activation of the footing sliding mechanism. Fig. 3 shows that stiffness degradation is more severe when the geometric ratio for shear H_e / B is lower, i.e., when the shear deformations are larger in comparison with the flexural ones. Also, normalization of the horizontal axis to the rotation of uplift initiation results in a contradictory, but otherwise expected, outcome regarding the relationship between *SF* and K_f / K_{f0} when compared with the results presented in [17]: the stiffness degradation becomes more intense as the static *SF* reduces. In fact, since the macro-element by Correia *et al*. [20] uses a more consistent approach for taking into account simultaneous uplift and inelasticity, it is expected that for larger *SFs* the behaviour is dominated by uplift response, with minor inelastic effects, whereas for lower *SFs* the response is dominated by hysteretic behaviour, thus leading to a faster stiffness degradation of the footing.

Another important point is the fact that, except for the case of H_e / B equal to one, stiffness degradation before uplift initiation is moderate to low ($K_f / K_{f0} \approx 0.75$-$0.95$) whereas it becomes much more significant after uplift initiation. Adopting performance criteria for foundation systems of $G / G_{max} \geq 0.3$ for the repairable damage limit state (as proposed in the Model Code for DDBD [23]) and assuming a linear relationship between the soil shear modulus *G* and the foundation rotational stiffness K_f, it is observed that the permissible rotation of the footing ranges from 4 to 10 times the rotation at uplift initiation, depending on H_e / B and *SF*.

In Fig. 4, a direct comparison between the curves derived by Paolucci *et al*. [17] and the curves derived herein is presented for H_e / B equal to 4. It is interesting to note that for small *SF* values the current curves fall below the ones of [17] whereas the opposite stands for high *SF* values. As explained above, this kind of difference was expected due to the more consistent approach for taking into account both uplift and inelasticity adopted in the macro-element of Correia *et al*. [20]. In fact, these results may indicate that the approach followed herein, along with the macro-element formulation that was used, attributes a more important role to inelasticity for low *SF* values than in the case of the existing curves. On the other hand, for large *SF* values inelasticity is less important and rocking prevails.

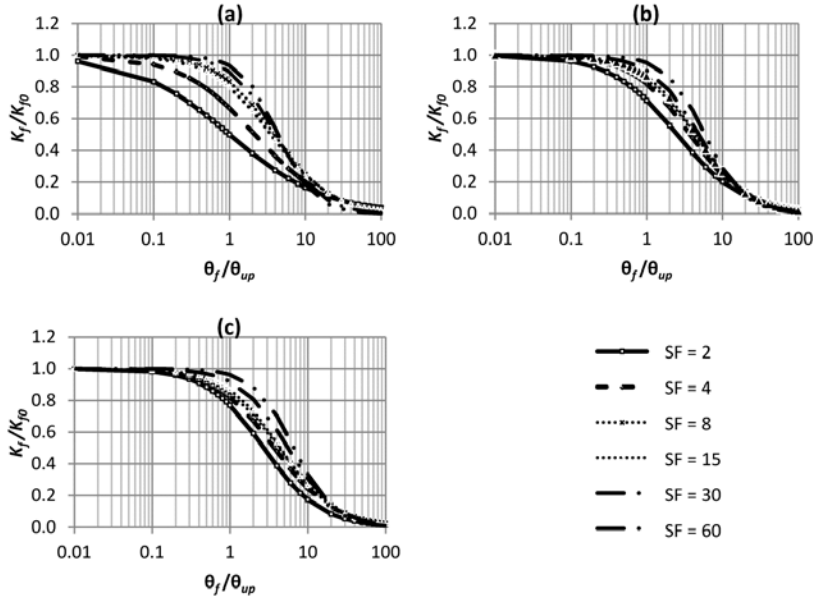

Fig. 3: Proposed stiffness degradation curves for (a) *He / B* = 1, (b) *He / B* = 2 and (c) *He / B* ≥ 3

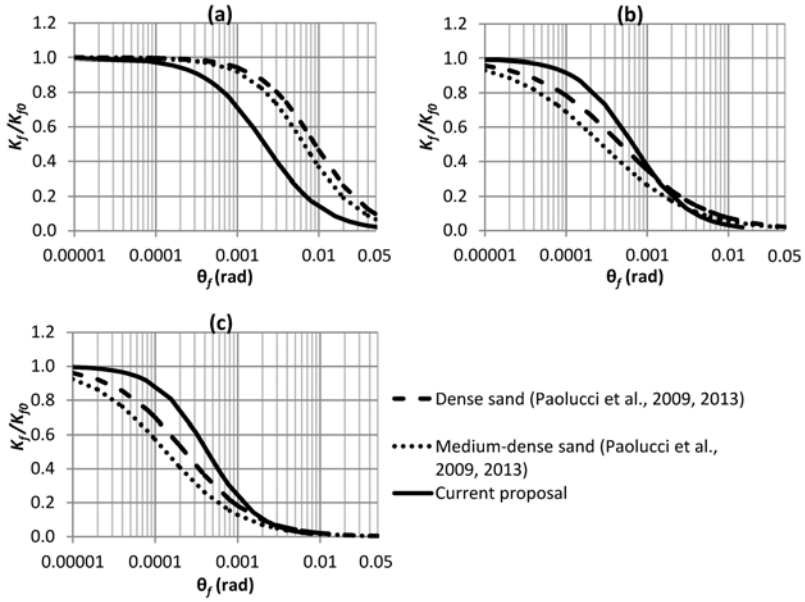

Fig. 4: Comparison between the proposed curves and the Paolucci *et al*. [17] stiffness degradation curves (*He / B* = 4): (a) *SF* = 2, (b) *SF* = 15 and (c) *SF* = 30

3.2 Equivalent viscous damping curves for cyclic loading

The energy dissipation mechanism for foundation systems on inelastic soil is represented herein in terms of EVD ratios. The cyclic loading analyses which were performed for deriving the stiffness degradation curves are also used for the calculation of the moment-rotation (M_f - θ_f) area-based EVD ratios. The area-based equivalent viscous damping concept computes a hysteretic component of EVD ratio, $\xi_{f,hyst}$, according to the area, A_h, of a stabilized hysteretic loop:

$$\xi_{f,hyst} = \frac{A_h}{2\pi F_m \Delta_d} \tag{5}$$

where F_m and Δ_d are the maximum force and maximum displacement attained within the cycle.

It should be noted that the EVD ratio calculated by this methodology is an estimate of the energy dissipation attributed to the inelastic deformation within the soil due to the loads transmitted by the superstructure and no other energy dissipation mechanisms, such as seismic wave radiation or nonlinear soil behaviour due to the passage of seismic waves, are included. Future research is needed to investigate different means of accounting for such energy dissipation and to develop expressions for spectral displacement reduction factors for foundation systems, as opposed to EVD expressions, for reasons provided in [24].

The hysteretic component of EVD ratios obtained from the cyclic loading analyses is shown in Fig. 5. Interestingly, higher damping values occur for low *SF* systems where plasticity seems to play a more significant role as explained earlier. Moreover, the EVD ratio showed a monotonic increase with rotation for such systems whereas for larger *SFs*, after a limit rotation was reached, the EVD ratio presented a descending trend with increasing foundation rotation. As explained above, the reason for this behaviour lies in the fact that the response of large *SF* systems is controlled by the non-dissipative uplift mechanism as soon as uplift initiates. Therefore, for small foundation rotations, plasticity dominates over uplift and hysteretic loops grow wider with increasing rotation, whereas after a limit rotation is reached, the hysteretic loops get narrower exhibiting low energy dissipation. Consequently, systems with very large *SF*, where uplift response is dominant, exhibit minor or practically no hysteretic damping. Nevertheless, it should be noted that the descending trend with increasing foundation rotation only occurs for values of rotation well beyond ten times the rotation at uplift initiation.

Considering the influence of geometric proportions, EVD ratios seem to increase as the H_e / B ratio decreases. The increase in EVD is more evident for intermediate values of *SF* and can be attributed to the hysteretic response in terms of shear force and activation of the sliding mechanism at the soil/footing interface. It should be noted that the recent macro-element approaches take into account the coupling of vertical, shear and moment responses, corresponding to a significant evolution from the SFSI representation by equivalent-linear uncoupled impedances [14-16, 20].

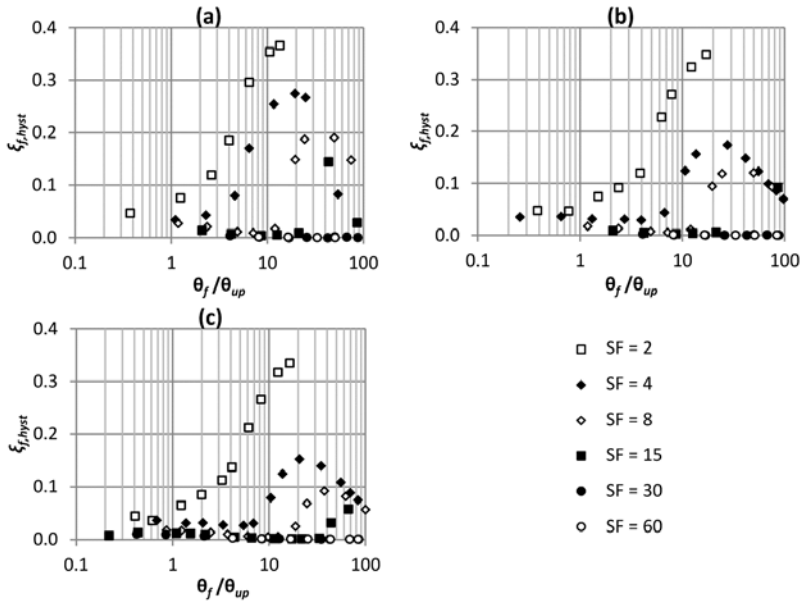

Fig. 5: Hysteretic component of the equivalent viscous damping ratio for shallow foundations with (a) *He / B* = 1, (b) *He / B* = 2 and (c) *He / B* ≥ 3

4. Design and response of structural wall buildings

This section applies the DDBD procedure, accounting for SFSI, to three case study buildings of 6, 8 and 12 storeys with height H_{tot}. The case study buildings consist of two RC C-shaped core walls, which are placed at the central part of the building and form the earthquake resisting system, along with RC frames which are designed to carry only gravity loads (see Fig. 6). A uniform storey height (h_{st}) of 3.3 m was adopted. Since the earthquake

resisting system consists of the core walls, only that part of the buildings was designed in this study. The wall geometric properties such as web length (l_w), flange length (l_f), wall thickness (b_w) and the storey mass (m) are presented in Table 1. Also, the foundation soil properties, namely the soil friction angle (ϕ') and the soil shear modulus (G), are given in Table 1. The Poisson's ratio (ν) was taken equal to 0.25 and the soil unit weight (γ) was considered to be 19 kN/m^3. Due to symmetry along the two horizontal axes, design information will be reported for only one of the two core walls. However, it is noted that both core walls share the same footing and that the footing height is equal to 1.60 m in all scenarios.

Table 1: Characteristics of the case study buildings

Building	# storeys	l_w/l_f (m)	h_{st}/H_{tot} (m)	b_w (m)	m_i (t)	N (kN)	ϕ'	G (MPa)
1	**6**	8.0/2.0	3.3/19.8	0.25	625/610*	5585	30º	60
2	**8**	8.0/2.0	3.3/26.4	0.25	625/610*	7620	32º	64
3	**12**	8.0/2.0	3.3/39.6	0.25	625/610*	12025	33º	90

*floor mass/roof mass

A comparison of the fixed and flexible-base approaches shows that when structural strain limits govern the design limit state (6-storey building), accounting for nonlinear SFSI leads to more flexible systems with lower base shear. However, in such cases the structural displacements increase and this may affect the performance of non-structural components during an earthquake. For taller buildings where code drift limits control the design, accounting for SFSI has led to stiffer systems (in the sense of secant stiffness to maximum displacement of the DDBD approach) with larger base shear and lower ductility demands. It results in larger reinforcement content both in flexure and shear, but the confinement reinforcement may be reduced.

Table 2: Comparison between the DDBD with fixed base and the DDBD with SFSI approaches

	# storeys	Δ_d (m)	μ_s	ξ_{sys} (%)	T_e (sec)	Drift (%)	V_b (kN)	B (m)	ρ_f (%)	SF	θ_f (rad)
Fixed base	**6**	0.284	7.58	17.3	2.75	2.2	4365	24.4	0.41	-	-
	8	0.423	6.54	17.0	4.06	2.5	3897	22.2	0.45	-	-
	12	0.589	4.14	15.7	5.47	2.5	4334	24.1	0.74	-	-
SFSI	**6**	0.312	7.58	15.9	2.91	2.4	4268	16.8	0.41	38.8	0.0010
	8	0.409	4.44	15.1	3.72	2.5	4423	18.0	0.55	37.3	0.0011
	12	0.591	3.71	16.1	5.53	2.5	5559	18.5	0.91	24.7	0.0020

The stark contrast between the two design approaches lies on the footing dimensions. At the beginning of the DDBD with SFSI iterative process it was intended to reduce the footing dimensions by mobilizing its bearing capacity. As it can be seen, the footing dimensions (B in Table 2) were reduced by 19% to 31%. In terms of concrete volume required for the footing construction, the reduction lies between 41% and 53%. As the required percentage of longitudinal reinforcement, ρ_f, for the footings designed considering SFSI is approximately equal to the footings designed as a fixed base, it is apparent that a significantly greater quantity of steel reinforcement is required for fixed-base footing solutions. It should be noted that the foundation pad reinforcement was sized taking into account possible overstrength of the wall (coming from actual reinforcement content and overstrength material properties), the range of which varied between 1.16-1.22 for fixed-base conditions and 1.15-1.20 for the SFSI approach.

In order to gauge the performance of the design solutions, nonlinear models of the walls were developed in Ruaumoko [25] with strength and stiffness properties set to match those obtained from the design, and these models were subjected to nonlinear time-history analyses (NLTHA) using a set of spectrum-compatible accelerograms. The walls were modelled using a lumped plasticity approach with Takeda thin hysteretic properties and unloading and reloading stiffness values in line with the recommendations of [1]. The nonlinear foundation response was modelled with a rotational and translational (horizontal) spring element since the software does not include the formulation of the macro-element used herein to develop the foundation response curves (K_f / K_{f0} and $\xi_{f,\ hyst}$ vs. θ_f). However, due to the large SF values and moderate rotations which were

assigned to the foundations of the case study buildings, their associated damping is negligible. Thus, it was deemed appropriate to model the foundation with a nonlinear elastic spring element both for the rotational and translational degrees of freedom, the properties of which were set in order to reproduce approximately the performance of the case study foundations derived from the macro-element in SeismoStruct [21]. Masses were lumped at each level of the structure and rigid diaphragm action was assumed. A tangent stiffness-proportional damping model was used, specifying 5% damping on the 2nd mode and a lower value on the 1st mode (in line with the recommendations from [1]). The gravity frames were not modelled at all since this research focuses on the response of the walls, but future research on the effect of wall rocking on the gravity frames is of interest.

Fig. 6 shows the peak displacements and drifts obtained for the case study structures designed considering the nonlinear SFSI effects. It can be seen that the displacement and drift profiles match the design objectives well, indicating that the DDBD with SFSI design methodology is very promising and that the SFSI effects can be successfully accounted for. In Fig. 6, the comparison between the inter-storey drifts of the fixed-base buildings and the buildings incorporating nonlinear SFSI is also exhibited. The inter-storey drift profiles were calculated from the average of the maximum responses of the case study buildings. As one can observe, the design solutions which allow for foundation nonlinearity exhibit lower values of inter-storey drift compared to the traditional fixed-base approach for the 6 and 8-storey buildings. This outcome suggests that the SFSI approach was a little conservative in these cases. However, for the 12-storey building the opposite is observed. For this case study building the foundation rotation assigned during the design phase was about twice that of the other two case study buildings, while at the same time the wall is more slender. Therefore, the foundation rotation during the earthquake causes additional oscillation to the wall which, due to the slenderness of the wall, results into slightly increased inter-storey drift ratios.

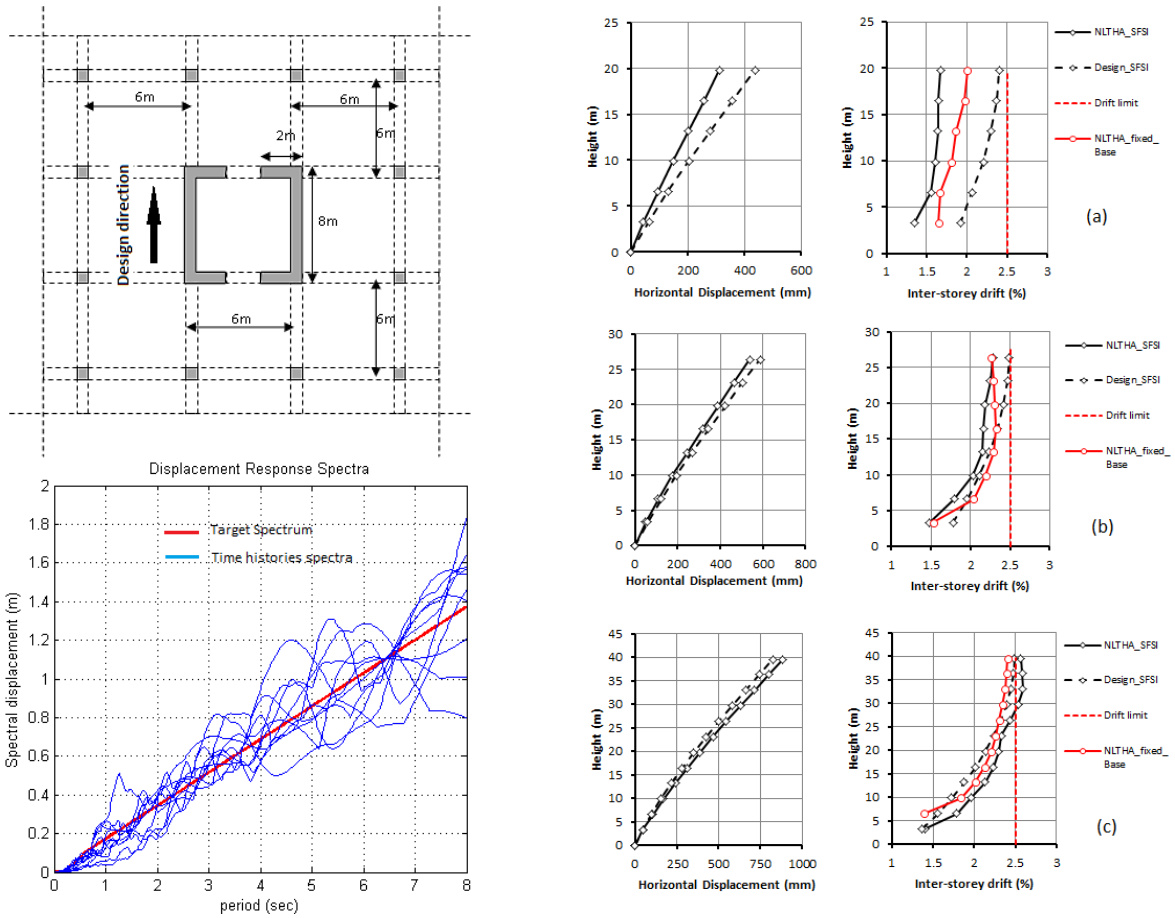

Fig. 6: Plan view of case-study buildings and displacement response spectra (left), and average (over 10 records) displacement and inter-storey drift profiles (right) of the (a) 6-storey, (b) 8-storey and (c) 12-storey building

In terms of maximum foundation rotation, the NLTHA results were found to significantly exceed the design objectives for the 6-storey (1.3 vs. 1.0 mrad) and 12-storey (3.5 vs. 2.0 mrad) buildings whereas for the 8-storey building the design foundation rotation was not exceeded (0.8 vs. 1.1 mrad). The differences may be due to the modelling of the nonlinear foundation in Ruaumoko [25] with a rotational and translational spring. In order to obtain more accurate results on the performance of the design solutions, NLTHA using the SFSI macro-element should be conducted in the future.

5. Conclusion

The focus of this paper has been the development of simple design methods able to account for the foundation flexibility and its nonlinear behaviour on the response of a structure with adequate accuracy. One of the main contributions of the research presented was the construction of shallow foundation response curves accounting for several nonlinear and coupled mechanisms (plasticity, uplift, soil/footing contact degradation, sliding, P-Δ effects) that take place during the response of shallow foundations under earthquake excitation through the use of a state-of-the-art macro-element formulation. Cyclic loading analyses were performed and stiffness degradation as well as equivalent viscous damping ratio curves were obtained for foundation systems with different static safety factors and shear ratio values. The newly obtained curves improve on existing curves in the literature since the effects of shear force and uplift were included.

The newly developed foundation response curves were implemented in an iterative DDBD process in order to develop an integrated design method for RC wall buildings and their foundations. Application of the DDBD to three case study wall buildings, with and without consideration of nonlinear foundation response, showed that when structural strain limits govern the limit state design (small to medium-rise buildings), accounting for SFSI leads to more flexible systems with lower base shear for the same structural ductility demand. For taller buildings, where code drift limits control the design, accounting for SFSI leads to stiffer structural systems (in the sense of secant stiffness to maximum displacement of the DDBD approach) with larger base shear and lower structural ductility demands. Accordingly, accounting for SFSI will affect the superstructure reinforcement detailing and the foundation dimensions. Buildings designed accounting for nonlinear SFSI are shown to require considerably smaller foundation dimensions with associated savings on materials likely.

The performance of the design solutions was checked via NLTHA and it was found that the displacement and drift profiles of the superstructure were adequately controlled by the design procedure. On the other hand, the results obtained for the case study structures suggest that future research should aim to better refine the means of controlling the foundation rotation demands and also further verify the performance of the method for structures possessing foundations with lower factors of safety.

References

[1] Priestley MJN, Calvi GM, Kowalsky MJ (2007): *Displacement-Based Seismic Design of Structures*. IUSS Press, Pavia, Italy.

[2] Mylonakis G, Gazetas G (2000): Seismic soil-structure interaction: Beneficial or detrimental? *Journal of Earthquake Engineering*, **4** (3), 277-301.

[3] Negro P, Paolucci R, Pedretti S, Faccioli E (2000): Large Scale Soil-Structure Interaction Experiments on Sand Under Cyclic Loading. *12th World Conference on Earthquake Engineering*, Auckland, New Zealand.

[4] Gajan S, Kutter BL, Phalen JD, Hutchinson TC, Martin GR (2005): Centrifuge modeling of load-deformation behaviour of rocking shallow foundations. *Soil Dynamics and Earthquake Engineering*, **25** (7-10), 773-783.

[5] Paolucci R, Shirato M, Yilmaz MT (2008): Seismic behavior of shallow foundations: Shaking table experiments vs. numerical modelling. *Earthquake Engineering and Structural Dynamics*, **37** (4), 577-595.

[6] Gajan S, Kutter BL (2008): Capacity, settlement, and energy dissipation of shallow footings subjected to rocking. *Journal of Geotechnical and Geoenviromental Engineering*, **134** (8), 1129-1141.

[7] Anastasopoulos I, Gazetas G, Loli M, Apostolou M, Gerolymos N (2010): Soil failure can be used for seismic protection of structures? *Bulletin of Earthquake Engineering*, **8** (2), 309-326.

[8] Drosos V, Georgarakos T, Loli M, Anastasopoulos I, Zarzouras O, Gazetas G (2012): Soil-foundation-structure interaction with mobilization of bearing capacity: Experimental study on sand. *Journal of Geotechnical and Geoenviromental Engineering*, **138** (11), 1369-1386.

[9] Pecker A (2003): Aseismic foundation design process. Lessons learned from two major projects: the Vasco da Gama and Rion-Antirion bridges. *5th International Conference on Seismic Bridge Design and Retrofit for Earthquake Resistance*, La Jolla, USA.

[10] Nova R, Montrasio L (1991): Settlements of shallow foundations on sand. *Géotecnique*, **41**, 243–256.

[11] di Prisco C, Nova R, Sibilia A (2003): Shallow Footings Under Cyclic Loading: Experimental Behaviour and Constitutive Modeling. *Geotechnical Analysis of Seismic Vulnerability of Historical Monuments*, Maugeri & Nova (eds), Pàtron.

[12] Paolucci R (1997) Simplified evaluation of earthquake-induced permanent displacements of shallow foundations. *Journal of Earthquake Engineering*, **1** (3), 563-579.

[13] Cremer C, Pecker A, Davenne L (2002): Modelling of nonlinear dynamic behaviour of a shallow strip foundation with macro-element. *Journal of Earthquake Engineering*, **6** (2), 175-211.

[14] Chatzigogos CT, Pecker A, Salençon J (2009): Macroelement modeling of shallow foundations. *Soil Dynamics and Earthquake Engineering*, **29** (5), 765-781.

[15] Chatzigogos CT, Figini R, Pecker A, Salençon J (2011): A macroelement formulation for shallow foundations on cohesive and frictional soils. *Int. Journal of Numerical and Analytical Methods in Geomechanics*, **35**, 902-931.

[16] Figini R, Paolucci R, Chatzigogos CT (2012): A macro-element model for non-linear soil-shallow foundation-structure interaction under seismic loads: theoretical development and experimental validation on large scale tests. *Earthquake Engineering and Structural Dynamics*, **41** (3), 475-493.

[17] Paolucci R, Figini R, Petrini L (2013): Introducing dynamic nonlinear soil-foundation-structure interaction effects in displacement-based seismic design. *Earthquake Spectra*, **29** (2), 475-496.

[18] Priestley MJN, Kowalsky MJ (2000): Direct Displacement-Based Design of Concrete Buildings. *Bulletin of the New Zealand National Society for Earthquake Engineering*, **33** (4), 421-444.

[19] Sullivan TJ, Salawdeh S, Pecker A, Corigliano M, Calvi GM (2010): Soil-foundation-structure interaction considerations for performance-based design of RC wall structures on shallow foundations. *Soil-Foundation-Structure Interaction*, Ch. 25, 193-200, Orense, Chouw & Pender (eds), Taylor & Francis.

[20] Correia AA, Paolucci R, Pinho R (2016): Shallow foundation macro-element for seismic soil-structure interaction analysis. *16th World Conference on Earthquake Engineering*, Santiago, Chile.

[21] Seismosoft (2013): *SeismoStruct: A Computer Program for Static and Dynamic Nonlinear Analysis of Framed Structures*, available from http://www.seismosoft.com, Pavia, Italy.

[22] Mylonakis G, Nikolaou S, Gazetas G (2006): Footings under seismic loading: Analysis and design issues with emphasis on bridge foundations. *Soil Dynamics and Earthquake Engineering*, **26** (9), 824-853.

[23] Sullivan TJ, Priestley MJN, Calvi GM (2012): *A Model Code for the Displacement-Based Seismic Design of Structures*. IUSS Press, Pavia, Italy.

[24] Pennucci D, Sullivan TJ, Calvi GM (2011): Displacement Reduction Factors for the Design of Medium and Long Period Structures. *Journal of Earthquake Engineering*, **15** (S1), 1-29.

[25] Carr A (2008): *Ruaumoko: The Maori God of Volcanoes and Earthquakes*. Civil Engineering Department, University of Canterbury, Christchurch, New Zealand.